Incorporation of a Solar Tracking System for Enhancing the Performance of Solar Air Heaters in Drying Apple Slices

Ramadan ElGamal [1] Sameh Kishk [1] Salim Al-Rejaie [2] Gamal ElMasry [1, 2, 3]

[1] *Agricultural Engineering Department, Faculty of Agriculture, Suez Canal University, 41522 Ismailia, Egypt*
[2] *Department of Pharmacology & Toxicology, College of Pharmacy, King Saud University, Saudi Arabia*
[3] *Institute of Agriculture and Food Research and Technology (IRTA), Finca Camps i Armet s/n, 17121, Monells, Spain (E-mail: gamal.masry@irta.cat)*

ABSTRACT

The main aim of this study was to develop an integrated solar-tracking system to maximize the efficiency of solar heaters manufactured from recyclable aluminum cans (RAC) for optimum drying of apple slices. The results revealed that the thermal efficiency of the solar air heater incorporated with a tracking unit was significantly improved by about 45% compared with the conventional fixed heaters at all tested air flow rates. The highest thermal efficiency of 87.1% of the solar air heater equipped with a tracking unit was achieved at the highest air flow rate of 44 m^3h^{-1}. The highest moisture diffusivity (D_{eff}) at the high levels of drying air temperature and flow rate and the highest value of D_{eff} (5.43×10^{-10} m^2s^{-1}) was obtained in the dryer with a tracking system at the highest air flow rate of 44 m^3h^{-1}. The drying rate of apple slices under such a tracking module was considerably higher than that of either the traditional fixed system or the ambient sun drying.

Keywords: Solar tracking; recyclable cans; apple; drying; solar dryer.

1. INTRODUCTION

Dehydration process of apples is nowadays a frequent practice to produce dried forms that can be consumed conveniently or be used as secondary raw materials for other subsequent processing (**Akpinar et al., 2003; Vega-Gálvez et al., 2012**). Although food dehydration and moisture reduction in the product has valuable advantages such as reducing the microbial activity and chemical deterioration besides the substantial reduction in the product volume (**Doymaz & Pala, 2003**), the drying of food products consumes a considerable amount of energy (**ElGamal et al., 2014; 2015**). Using renewable solar energy in drying process reduces the use of conventional energy sources and as a result reduces the pollutant emissions (**Santos et al., 2005**). Solar energy as the cleanest source of energy is also easily accessible and abundantly available as an alternative energy source in nature **(Rao et al., 2017)**. Using solar drying for food preservation is one of the most optimistic applications of solar energy **(Sekyere et al., 2016**). Indirect solar drying systems (solar dryers with a solar air heater) provide better control of the characteristics of the drying air (**Sacilik et al., 2006; Sreekumar et al., 2008**).

The performance of any solar system such as solar air heaters and solar panels depends fundamentally on the intensity of the solar radiation and the incidence angle. Maximum energy is produced by a solar system when it is positioned at right angle to the sun **(Yousef, 1999; Khan, 2010)**. Moving the solar system to continuously face the sun radiation during the whole day is an efficient approach to achieve the maximum efficiency of solar collection compared to the fixed solar systems. To achieve high system efficiency, an automated system (namely solar tracker) is required to continually adjust the system to the optimum position as the sun traverses the sky. Commercial purposes of solar tracking systems are (1) increasing solar system output, (2) improving the thermal efficiency, (3) maximizing the power per unit area and (4) grabbing the energy throughout the day. The theoretical background and intensive details for different solar trackers and their operating systems can be found in **Banerjee (2015)**. Numerous experiments performed in employing solar tracking systems revealed that up to 40% of additional energy can be attained **(Clifford and Eastwood, 2004)**. Studies showed also that tracking systems increased pumping capacity **(Bione et al., 2004)**, power collection efficiency (**Rizk and Chaiko, 2008**) and thermal efficiency (**Guihua et al., 2012; Dhanabal et al., 2013)** over the fixed-angle system. Moreover, reports indicated that the use of solar trackers can increase electricity production by about 15-35% (**Tiberiu et al., 2012; Anyaka et al., 2013**; **Miloudi et al., 2013; Quesada et al., 2015; Watane and Dafde, 2013**) and up to 40% in some regions (**Mork and Weaver, 2009; Banerjee, 2015)** compared with solar modules of a fixed orientation angle. For instance, **Anusha et al. (2013)** compared the fixed and single axis solar tracking systems for six days and their results show that the solar tracking system increased the efficiency of about 40% and the energy received was improved from 9.00 to 18.00 h.

Despite such confirmed merits of using solar trackers for improving the performance of solar systems (**Samimi-Akhijahani, & Arabhosseini, 2018; Devan et al., 2020**), incorporating solar trackers with solar air heaters especially in drying agricultural products has received little attention for practical applications. Thence, the main aim of this study was to develop an integrated solar tracking system to maximize the conversion efficiency of the previously designed recyclable aluminum cans (RAC) solar air heater by continually adjusting its direction to the optimum angle towards the sun during daytime hours. The thermal efficiency of the fixed and tracking solar collectors was explored at different air flow rates and the drying behavior of peeled and unpeeled apple slices in both systems was investigated and compared with the traditional ambient sun drying.

2. MATERIALS AND METHODS

2.1. Solar dryer

In our previous study **(Kishk et al., 2019)**, an indirect solar dryer with forced convection was designed and constructed at our lab in Suez Canal University, Egypt. In essence, the solar air heater was fabricated from recycled aluminum cans (RAC) through which the ambient air was heated and then forced inside drying cabinets. The RAC solar air heater was orientated in the East-West direction as the best orientation in Ismailia city, Egypt (latitude of 30.62º, longitude 32.27º). The solar heaters were placed facing south and inclined at an angle of 31º and kept in such a fixed position during the whole drying process.

In the current study, a solar tracking unit was developed to be incorporated with an RAC air heater in order to maximize its conversion efficiency by continually adjusting its orientation angle during the experiments. A drying cabinet to accommodate food samples to be dried was then attached to each air heater (The fixed and tracking ones). Two photovoltaic panels were also installed on the tracking system to provide the required power for operating air blowers and the motor of the tracking system itself as shown in Figure (1). The detailed information about the design of the RAC solar air heater was explained in details by **Kishk et al. (2019).**

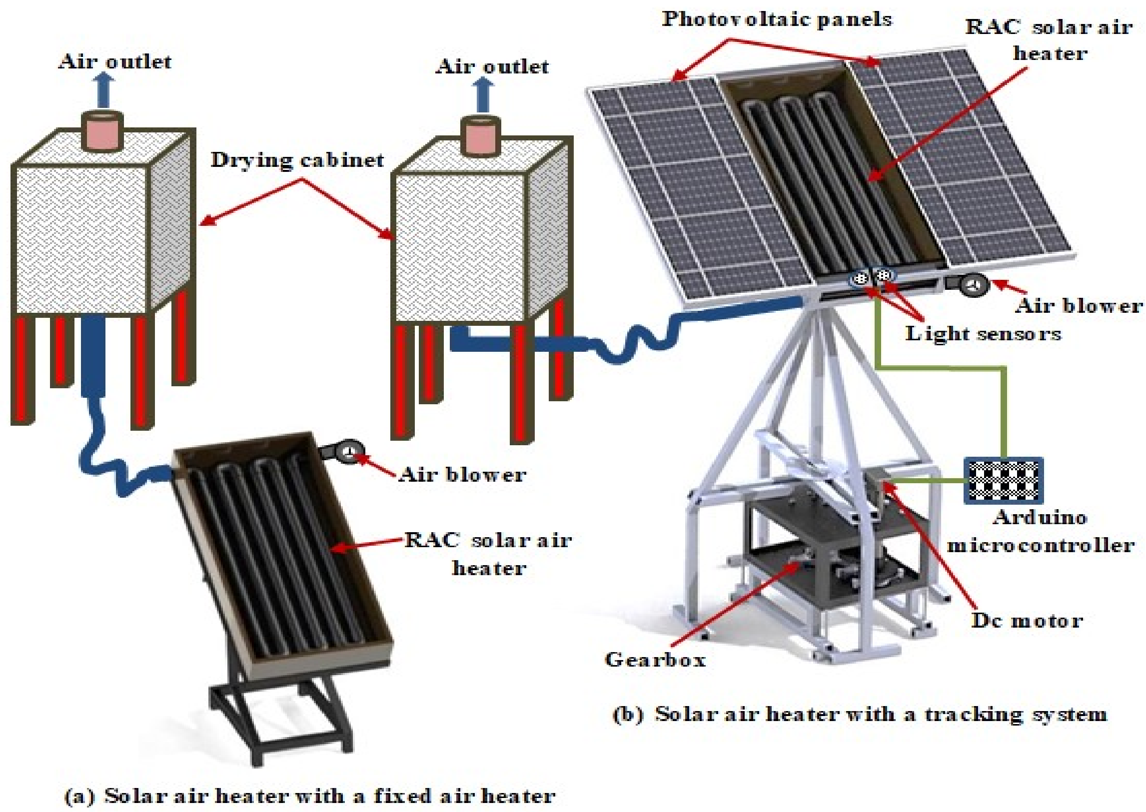

Figure 1a. Schematic diagram for solar dryers integrated with solar air heaters at (a) fixed orientation (left side) and (b) attached with a solar tracking unit (right side).

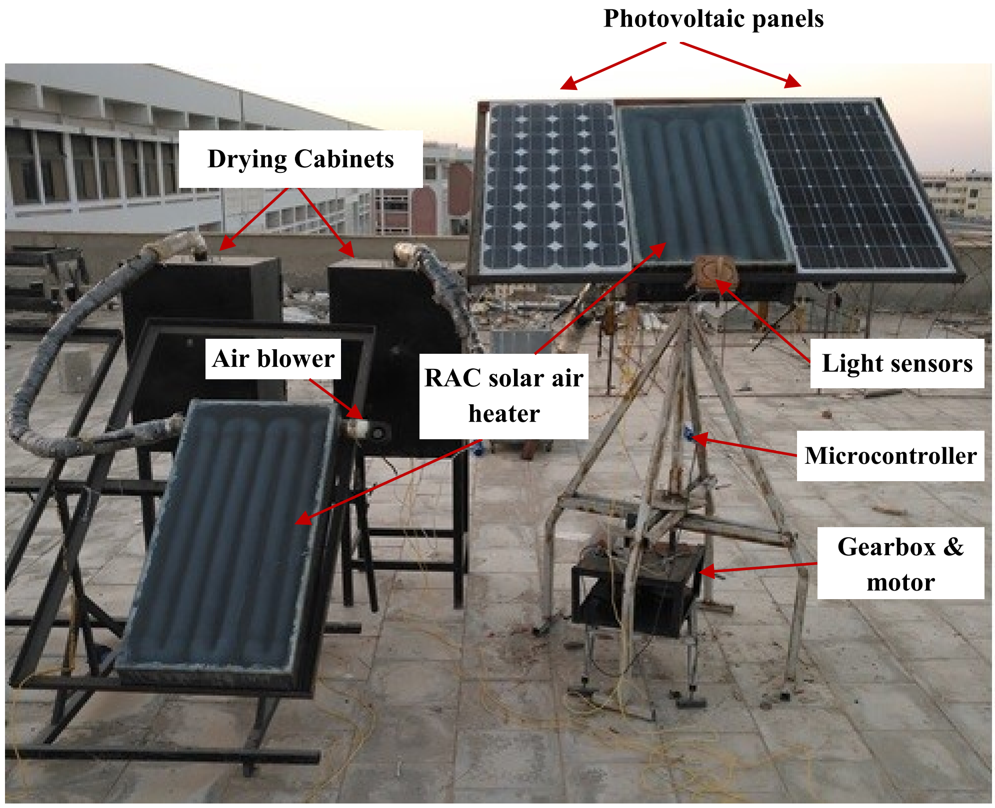

Figure 1b. A photograph of solar air heaters integrated with drying cabinets

2.2. Solar tracking system

A single-axis tracking unit with one axis of rotation was particularly developed to be incorporated with the solar air heater. The two solar panels as well as the solar heater were fixed on the upper end of an iron shaft of the axis of rotation and the other end of the shaft was attached to the biggest gear in the gearbox to reduce the rotational speed incoming from the motor as the required movement step was very small in each cycle. The tracking module consists of light sensing devices, a control unit, and a driving mechanism as shown in Figure (1). Two light sensors were attached to the forefront frame of the solar collector (Figure 1) to measure the light intensity received from the sun. The solar collector of the air heater will remain in a certain position when light intensity received by both light sensors is equal. If light intensity received by one sensor was different from the other sensor (due to movement of the sun), it means the sun moved to a new position and the whole collector should be rotated to face the sun in this new position. The signals from light sensors were transferred to a microcontroller unit to operate the DC motor of a driving mechanism for moving the solar air heater to this new position. The driving mechanism supported with a differential gearbox and driven by the DC motor was responsible for moving the whole unit to a new position until both sensors receive equal light intensity again.

2.3. Experimental setup

Drying of apple slices using a fixed and a tracking solar air heater system was conducted during July, 2019 under clear climate conditions. Three experimental runs were conducted for drying apple slices (var. Red delicious) under three air flow rates of 22, 33 and 44 m^3h^{-1}. Before conducting each experiment, fresh apple fruits were washed by running water and some fruits were peeled before being sliced. The peeled and unpeeled apples were cut horizontally into slices with approximately 6.0±1 mm in thickness. To prevent browning of apples slices prior to solar drying, all raw slices were immersed in ascorbic and citric acid solution (10 g ascorbic acid + 2 g citric acid dissolved in one liter of distilled water) (**Pizzocaro et al., 1993**). Apple slices were then kept on a mesh grid for 5 min at the room temperature (25 °C) to drain all excessive immersion solution before being dried in the dryers. The slices were arranged over 50 × 50 cm trays in four rows (2 rows of peeled slices and 2 rows of unpeeled slices) with a net weight of about 300 g for each tray. Three trays full of apple slices were prepared for each experimental run: two trays to be dried inside the fixed and tracking solar dryers besides one tray was used for traditional sun drying (control). Before each experimental run, the desired air flow rate was adjusted using a digital blower speed controller (SMB-10, USA). The experimental work was run for 10 hours continuously through the period from 8 am to 6 pm, solar time. During the experimental work, an electrical digital balance (BS-Series, China) with an accuracy of 0.001 g was used to determine the mass of wet and dry samples to calculate moisture content. The temperature and the relative humidity of the drying air were continuously recorded during the experiments using a data logger (Lab-Jack logger, USA) connected with a computer supported with instantaneous data acquisition software (Weather link, USA). The output data were recorded every five minutes and averaged every one hour. Climate conditions such as air speed, solar radiation and dew-point temperature were recorded by a meteorological station (Vantage Pro 2, Davis, USA) installed in the experimental location. Moreover, a pyranometer was used for measuring the solar irradiance at the collectors and expressed as flux density (W/m^2). The technical specifications for all devices used in this study are presented in Table 1.

Table 1. Technical specifications of the used instrumentations and measurement devices.

Device or instrument	**Quantity**	**Technical specifications**
Photovoltaic panels	2	Maximum power = 300W each Power voltage = 12V
Tracking motor	1	DC motor, 12V, 50W
Air blower	2	DC fan, 12 V, 40W
Light sensors	2	Lab designed
Anemometer	1	SMB-10, USA, measuring range up to 30 ms^{-1} and accuracy of ± 0.1 ms^{-1}
Thermocouples	8	K-type -200:1200 °C ±0.5 °C
Data logger	1	Lab-Jack logger, USA
Digital balance	1	BS-Series, China, with an accuracy of 0.001 g

2.4. Thermal efficiency determination

To examine the effectiveness of using the solar tracking system for improving the performance of the RAC solar systems, thermal efficiency was determined under the tested air flow rates. Thermal efficiency of the solar heating systems (η) was calculated using the following equation **(Kishk et al., 2019)**:

$$\eta = \frac{\dot{m} \cdot C_{p}(T_0 - T_i)}{I \cdot A_c} \qquad (1)$$

where: $\dot{m}$ is the air mass flow rate (kg s^{-1}), C_p is the specific heat of the air (J Kg^{-1} K^{-1}), T_o is the outlet air temperature (K), T_i is the inlet air temperature (K), I is the total solar radiation incident upon the plate of the solar collector (Wm^{-2}), and A_c is the area of collector (m^2).

2.5. Drying process and data analysis

To obtain the drying curves of apple slices, samples of peeled and unpeeled apple slices were weighed before drying and constantly monitored at different times during drying experiments to record weight loss. The initial moisture content of apple samples determined using the oven-drying method (**Zlatanović et al., 2013**) was 86.12% wet basis (6.2 kg water/kg dry matter). Based on the initial moisture content and weight loss data recorded during drying process in both systems, the moisture content of apple slices at various stages during drying operation can be easily estimated. Due to the fluctuation of the drying air temperature during solar drying process, the average drying rate can be determined from the following formula at every tested flow rate of the drying air using the measured values of moisture contents:

$$DR = \frac{M_0 - M_f}{\Delta t} \qquad (2)$$

where DR is the average drying rate (kg H_2O/kg dry solids/hour), M_0 and M_f are the initial and final moisture contents (kg water/kg dry matter), respectively, Δt is the drying period (10 h).

2.6. Estimation of effective moisture diffusivity (D_{eff})

As declared in Eq. 3, Fick's second law of diffusion can be used to explain the drying process of apple since moisture diffusion across the spatial dimension (Z) is one of the main mass transfer phenomena that describes drying process of agro-food materials (**Doymaz, 2007**).

$$\frac{\partial MR}{\partial t} = D_{eff}\frac{\partial^2 MR}{\partial Z^2} \qquad (3)$$

The moisture ratio (*MR*) that relates the gradient of the sample moisture content at a certain time (M_t) to both the initial (M_0) and the equilibrium moisture contents (M_e) can be calculated using Eq. 4.

$$MR = \frac{M_t - M_e}{M_0 - M_e} \qquad (4)$$

where D_{eff} is the effective moisture diffusivity ($m^2\ s^{-1}$), M_t is the moisture content at a time *t* of drying (kg water/kg dry matter), M_e is the equilibrium moisture content (kg water/kg dry matter). The value of the equilibrium moisture content is relatively small compared to M_t or M_0. Thus equation 4 can be safely simplified to $MR=M_t/M_0$ (**Doymaz & Pala, 2003; Kishk et al., 2019**).

Assuming that temperature and diffusion coefficients are constant during drying, moisture migration is only caused by diffusion and shrinking is negligible, thus, the solution of Fick's law for a thin plate (apple slice) can be given as follow (**Baroni & Hubinger, 1998**):

$$MR = \frac{8}{\pi^2}\sum_{n=0}^{\infty}\frac{1}{(2n+1)^2} exp\left[-\frac{(2n+1)^2\pi^2 D_{eff}t}{4L^2}\right] \qquad (5)$$

where *L* is the half thickness of slab (m) and *n* is the number of terms in the diffusion cycles. As the thickness of the apple slice was quite small (0.006 m) and the drying time was relatively large, Eq. (5) can be further simplified to only the first term ($n = 0$) of the series (**Tutuncu & Labuza, 1996**). Hence, Eq. (5) is rewritten in a logarithmic form as follows:

$$ln\, MR = ln\, \frac{8}{\pi^2} - \frac{\pi^2 D_{eff}t}{4L^2} \qquad (6)$$

Therefore, the slope of the linear relationship between the dependent variable ($f(t) = ln\, MR$) and the drying time (t) was then used to estimate the effective moisture diffusivity (D_{eff}) according to Eq. (7):

$$Slope = -\frac{\pi^2 D_{eff}}{4L^2} \qquad (7)$$

2.7. Drying models

Mathematical modeling is an important step in proper design of the dryers to better understanding the mechanism of drying processes. Page model (**Velić et al., 2004; Kaleta et al., 2013**) as well as Henderson & Pabis model **Zlatanović et al. (2013)** were used to describe the drying kinetics and the changes in moisture content of apple slices during drying process:

Page model: $$MR = \exp(-kt^n) \qquad (8)$$

Henderson & Pabis model: $$MR = a\exp(-kt) \qquad (9)$$

The parameters *k, n* and *a* were calculated by using least squares regression solved by a Quasi-Newton numerical method. The correlation coefficient (R^2), reduced chi-square (χ^2) and root mean square error (*RMSE*) were used as measures of model robustness (**Kishk et al., 2019**).

3. RESULTS AND DISCUSSION

During drying period, the ambient air temperature ranged from 32 to 38 °C with relative humidity values ranged from 40 to 60 %. The solar radiation values varied during the drying period where the minimum values recorded was observed at the beginning and at the end of the drying time (8 am and 6 pm) with a minimum value of 220 Wm^{-2}. Meanwhile, the maximum values of the solar radiation were recorded at noon (11-1 pm) with a minimum value of 870 Wm^{-2}. Figure 2 illustrates the variation of air temperature of the ambient and drying air in the fixed and tracking systems at different air flow rates of 22, 33, 44 m^3h^{-1}. It is quite clear that the solar air heater equipped with a tracking unit heats up the air to temperatures higher than that in the fixed solar air heater at all tested air flow rates. This implies that the tracking system maximized the benefits from the solar radiation incident on the solar collector resulting in higher air temperatures during the whole drying period.

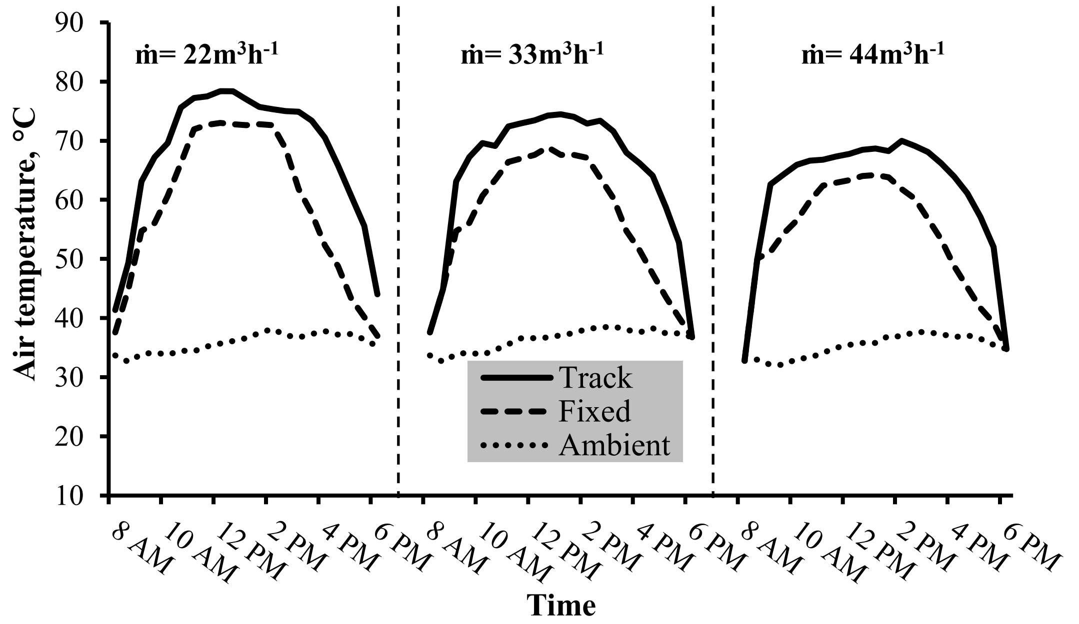

Figure 2. Variation of air temperature during the drying time at different air flow rates (22, 33, 44 m^3h^{-1}).

It can be also seen from Figure 2 that the outlet air temperature decreased as the air flow rate increased. For example, the maximum temperature of the outlet air from the fixed solar heater was 72.8, 68.9, 64.2 °C at the air flow rate of 22, 33 and 44 m^3h^{-1}, respectively. Similarly, the maximum temperature of the outlet air from the tracking solar heater reached 78.5, 74.4, 70.0°C at the air flow rate of 22, 33 and 44 m^3h^{-1}, respectively (Figure 2). This might be ascribed to the longer residence time for the air inside the solar collector at lower air flow rates (**Alta et al., 2010; Kishk et al., 2019**).

3.1. Thermal efficiency

The thermal efficiency of the fixed and tracking solar heaters was calculated according to equation (1) based on the temperature and weather data recorded during the drying experiments at different air flow rates and the results are presented in Table 2. It is clear that the thermal efficiency of the solar air heater was enhanced significantly to about 45% when the tracking system was used. At all tested air flow rates, the solar air heater with a tracking system provided higher thermal efficiency than the fixed solar air heater. For example, at the air flow rate of 22 m^3h^{-1}, the average thermal efficiency realized by the fixed solar air heater was 35%. Meanwhile, the average thermal efficiency increased up to 50.9% with heaters equipped with a tracking system at the same air flow rate (Table 2).

The results also showed that as the airflow rate increased the thermal efficiency of the solar air heater substantially improved (Table 2). For example, when the airflow rate increased from 22 to 44 m^3h^{-1}, the average thermal efficiency of the fixed solar air heater augmented from 35 to 56.1%, respectively. Meanwhile, the corresponding values of the average thermal efficiency of the solar air heater with a tracking system increased from 50.9 to 80.7% when air flow rate increased from 22 to 44 m^3h^{-1}, respectively. This trend of the results is in agreement with those of the previous studies reported for the RAC solar air heaters (**Ozgen et al., 2009; Kishk et al., 2019**).

Table 2. Thermal efficiency (%) of the fixed and tracking solar air heaters operated at different air flow rates.

System	**$\dot{m}$ = 22 m^3h^{-1}**		**$\dot{m}$ = 33 m^3h^{-1}**		**$\dot{m}$ = 44 m^3h^{-1}**	
	Fixed	**Tracking**	**Fixed**	**Tracking**	**Fixed**	**Tracking**
Min	15.6	44.8	24.4	60.8	27.3	71.0
Max	42.6	61.0	54.1	75.4	64.2	87.1
Average	**35.0**	**50.9**	**47.3**	**68.3**	**56.1**	**80.7**

3.2. Drying process of apple slices

Apple slices were dried for 10 hours (from 8am to 6pm) inside solar dryers operated under fixed and tracking solar air heaters as well as in the ambient air (control). The experiments were repeated under different air flow rates of 22, 33, 44 m^3h^{-1}. The resulted drying curves of apple slices were then illustrated as shown in Figure 3. As a general trend, the drying rate of apple slices (either peeled or unpeeled) in the tracking unit was considerably higher than those in either fixed system or the ambient sun drying. For instance, after 10 hours (*i.e.* 600 min) of drying at the airflow rate of 22 m^3h^{-1}, the moisture content of the peeled apple slices decreased from 86.12% w.b. to 7.7 % w.b. for the tracking system; while, at the same air flow rate the final moisture content after the same period was still at 16.9 and 18% w.b. for the fixed system and the ambient drying, respectively. The high drying rate of apple slices realized in the tracking system could be ascribed to the higher temperature values of the drying air passed from the solar heater to the drying cabinet compared to those in the fixed ambient systems as illustrated in Figure 2. In essence, when drying temperature increased the effective moisture diffusion increased resulting in higher drying rate as explained later in section 3.4. Although apple slices were dried faster in the tracking system and eventually reached constant moisture content earlier, the system were kept working for the whole drying hours (*i.e.* 10 h) to facilitate the comparison with the other two drying systems operated at the same drying period (Figure 3).

On the other hand, Figure 3 shows that the drying curves of apple slices in the fixed solar heater and in the open sun drying (control) were close to each other at the lower air flow rate (*i.e.* 22 m^3h^{-1}). The drying rate of apple slices in the fixed system was higher than that of the ambient unit by increasing airflow rate as shown in Figure 3. These findings agree with those reported in our previous study on tomato drying (**Kishk et al., 2019**). This implies that the fixed solar air heater is not preferred to be used in drying applications at low air flow rates without improving the heater's thermal efficiency by employing different scenarios such as incorporating a tracking system. In all cases, the drying curves of apple slices (either peeled or unpeeled) within the tracking system were much better than that of the fixed and the control dryers under all values of air flow rates. This implies that dryers equipped with a tracking system have higher thermal efficiency and consequently will have efficient drying capacity of apple slices.

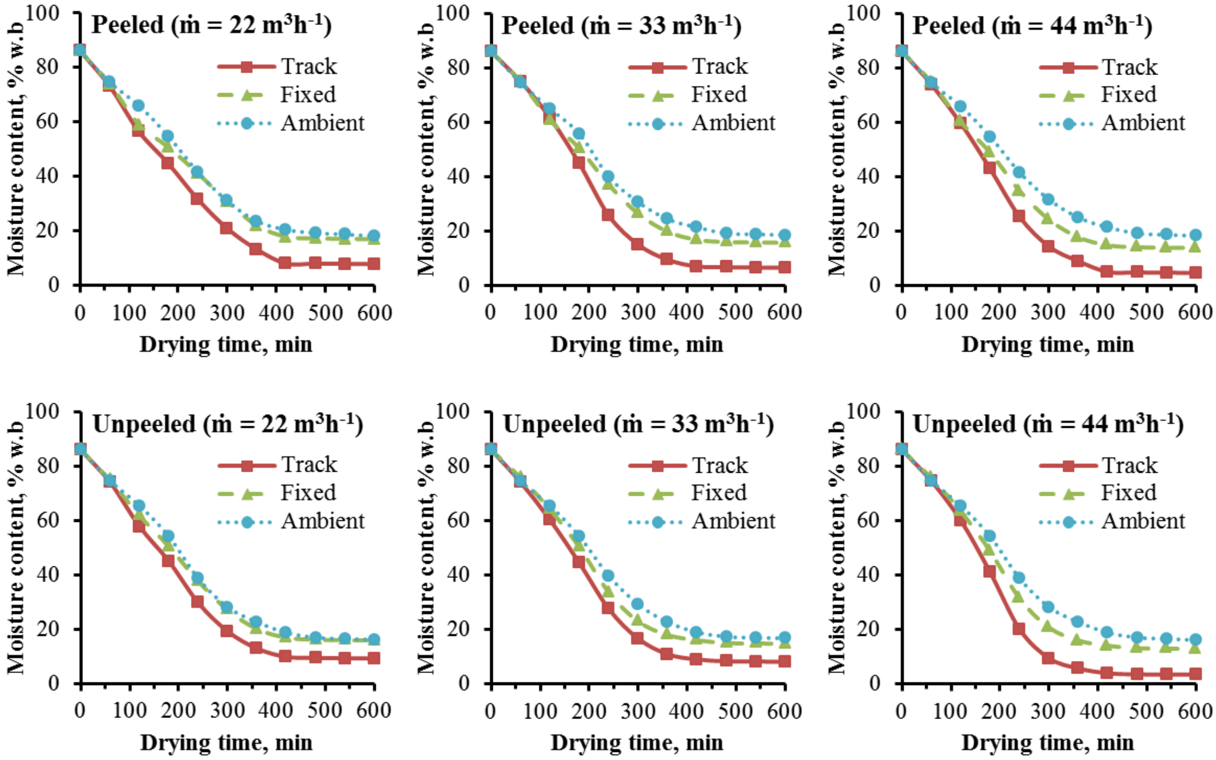

Figure 3. Drying curves of peeled and unpeeled apple slices dried in three drying systems (tracking, fixed and ambient) at different air flow rates.

To demonstrate the influence of air flow rate on the drying behavior of apple slices, Figure 4 presents the drying curves of unpeeled apple slices at different air flow rates for the fixed and tracking systems (same trend showed for peeled slices). For comparing drying behavior of apple slices using different drying systems at different air flow rates, the average drying rate *DR* (kg H_2O/kg dry solids/hour) defined as the difference between the initial and final moisture contents (kg H_2O/kg dry solids) divided by the drying time (10 h) was calculated and the results are tabulated in Table 3. In general, when the air flow rate increased, the drying rate also increased in both tested systems. Although the air temperatures delivered from the solar heaters were lower at higher flow rates (Figure 2), the dry air mass at high flow rates helped in removing the evaporated moisture from the apple slices quickly resulting in a higher drying rate. The increase of air flow rate from 22 to 33 m^3h^{-1} slightly increased the drying rate from 0.610 to 0.611 (kg H_2O/kg dry solids/hour) for tracking system and from 0.601 to 0.603 (kg H_2O/kg dry solids/hour) for fixed system as shown in Table 3. Meanwhile, further increase in the air flow rate from 33 to 44 m^3h^{-1} resulted in a considerable increase in the drying rate within the tracking system from 0.611 to 0.617 H_2O/kg dry solids/hour. As a consquence, the mositure content of apple slices at the end of drying period (10 working hours) in the tracking system was much lower compared to that in the fixed system for all trested flow rates as explicitly depicted in Figure 4. For instance, moisture content of apple slices dryied in the tracking system at a flow rate of 44 m^3h^{-1} reached 3.3 % at the end of the drying period compared to only 12.8% in the fixed system operated at the same flow rate. The same trend was also observed in the other tested flow rates as shown in Figure 4.

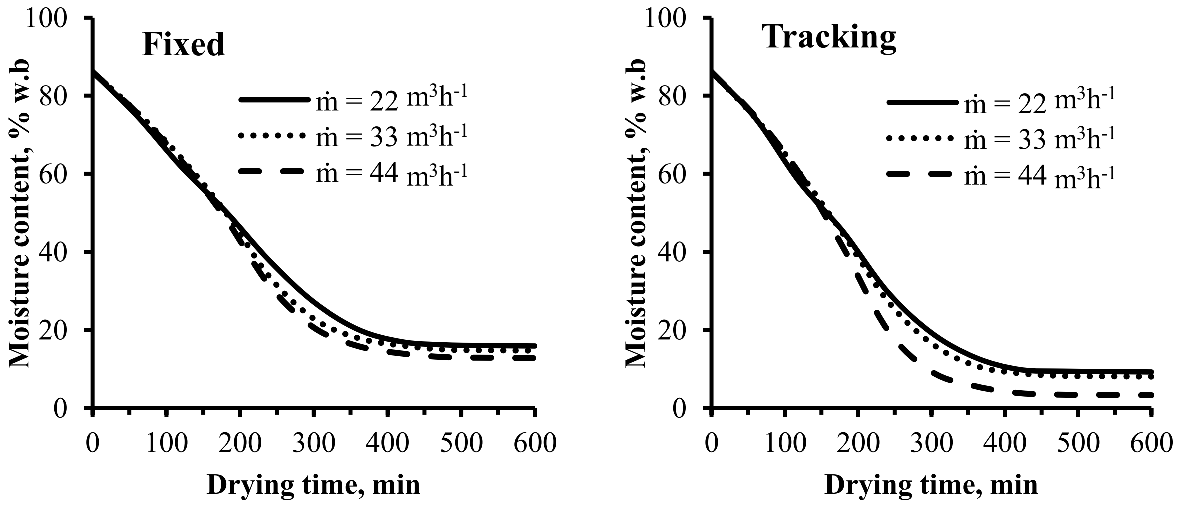

Figure 4. Effect of air flow rate on drying behavior of unpeeled apple slices for fixed and tracking drying systems

Table 3. Average drying rate *DR* (kg H_2O/kg dry solids/hour) of apple slices

Setup	System	Unpeeled slices		Peeled slices	
		Tracking	Fixed	Tracking	Fixed
1	$\dot{m} = 22\ m^3h^{-1}$	0.6103	0.6015	0.6121	0.6001
	Ambient*	0.6011		0.5995	
2	$\dot{m} = 33\ m^3h^{-1}$	0.6117	0.6032	0.6135	0.6018
	Ambient*	0.6004		0.5987	
3	$\dot{m} = 44\ m^3h^{-1}$	0.6170	0.6058	0.6156	0.6044
	Ambient*	0.6014		0.6001	

*The ambient drying was conducted under the ambient air conditions of temperature and air speed.

Analysis of variance (ANOVA) was conducted for each individual system first to see the difference in drying rate between peeled and unpeeled apple slices. Another ANOVA test was performed to see the difference in drying rate among the three drying systems (tracking, fixed and ambient) at different flow rates (22, 33 and 44 m^3h^{-1}). The analysis of variance (ANOVA) tests showed that there was no significant difference ($p \geq 0.05$) in drying rate for peeled and unpeeled apple slices dried in three drying systems at all tested conditions. These results are in agreement with **Defraeye and Radu (2018)** who reported that the peel is a barrier for moisture transport as a result of the reduced surface area for evaporation, but it is not a barrier for heat transport. However, they found that the differences between the peeled and unpeeled apple slices during drying were quite small due to the fact that the moisture below the peel can also escape partially via the side surface. This result was due to the small thickness of the slices used in their study (5mm) similar to the current study (6mm). For thicker apple slices, the impact of the peel is expected to become more pronounced. Paradoxically, there was a significant difference ($p \leq 0.05$) in drying rate among the three modes of drying as well as among the different air flow rates (Table 3). Least significant difference (LSD) test was used to compare drying rate of the three examined systems. From Table 3, one can also conclude that at a certain air flow rate, the drying rate of apple slices in the tracking system was significantly different ($p \leq 0.05$) than that in the fixed one. However, drying in the fixed system at low air flow rate 22 m^3h^{-1} showed no significant difference with the ambient air drying. For a given drying system, the drying rate at air flow rate of 44 m^3h^{-1} was significantly higher than the drying rate at the other tested air flow rates (22 and 33 m^3h^{-1}) and this was reflected in the moisture content curves shown in Figure 3 and Figure 4.

3.4. Moisture diffusivity

To analyze mass transfer phenomenon during drying process, it was important to investigate the condition of the effective moisture diffusivity (D_{eff}, $m^2\ s^{-1}$) because this feature affects the rate of water vapor transfer from inside the slice to its surface and because it represents most of the parameters influencing the drying rate (equation 5). The values of effective moisture diffusivity of apple slices during drying are tabulated in Table 4. The values of D_{eff} reported in this study as shown in Table 4 are in the range of those values reported for different cultivars of apple and different drying scenarios. The reported D_{eff} values lie between $1.7\times10^{-10} - 4.4\times10^{-10}$ m^2s^{-1} for apple *cv. Jonagold* (**Velić et al., 2004**), $0.48\times10^{-10} - 2.02\times10^{-10}$ m^2s^{-1} for apple *cv.* Red Delicious (**Kaya, 2007**) and $0.32\times10^{-10} - 1.53\times10^{-10}$ m^2s^{-1} for apple *var. Granny Smith* (**Vega-Gálvez et al., 2012)**. As a general trend in both fixed and tracking drying systems, the moisture diffusivity of peeled and unpeeled apple slices increased with increasing the air flow rate as shown in Table 4. The values of moisture diffusivity of apple slices dried in solar dryer equipped with a tracking system were significantly higher than those in the fixed solar dryer and ambient drying. The highest value of D_{eff} (5.43×10^{-10} $m^2\ s^{-1}$) in apple slices was obtained in the solar dryer equipped with a tracking system at the highest air flow rate (44 m^3h^{-1}), while the lowest value of D_{eff} (2.42×10^{-10} m^2s^{-1}) was recorded for the peeled slices dried in the ambient air.

Table 4. Effective moisture diffusivity $D_{eff} \times 10^{-10}$ [m^2s^{-1}] of apple slices during drying in different drying systems.

Setup	System	Unpeeled slices		Peeled slices	
		Tracking	Fixed	Tracking	Fixed
1	$\dot{m} = 22\ m^3h^{-1}$	3.60	2.69	3.92	2.56
	Ambient*	2.65		2.46	
2	$\dot{m} = 33\ m^3h^{-1}$	3.86	2.84	4.27	2.71
	Ambient*	2.61		2.42	
3	$\dot{m} = 44\ m^3h^{-1}$	5.43	3.08	4.84	2.92
	Ambient*	2.65		2.43	

*The ambient drying was conducted under the ambient air conditions of temperature and air speed.

As the effective moisture diffusivity is sensitive to any change in the drying parameters **(Zlatanović et al., 2013)**, the variation in the drying air temperatures among the examined drying systems (Figure 2) resulted in different values of moisture diffusivity of apple slices in these systems (**Diamante, 1994**). Figure 5 shows the relationship between the moisture diffusivity and the drying rate of apple slices in different drying systems. It is clear to observe that drying rate increases with the increase of moisture diffusivity in all tested drying systems. Apple slices in the tracking system had the highest values of moisture diffusivity, and as a result, the highest values of drying rate as shown in Figure 5. The highest values of moisture diffusivity realized in the tracking system could be ascribed to the higher temperature values of the drying air passed from the solar heater to the drying cabinet compared to those in the fixed system and the ambient sun drying. In essence, when the drying temperature increased, the moisture diffusion of agricultural products increased resulting in higher drying rate (**Doymaz, 2007; Brooks et al., 2008; Vega-Gálvez et al., 2012; Kishk et al., 2019)**. It is also important here to highlight the effectiveness of the tracking system for providing the highest values of D_{eff} and drying rate. Most importantly, the high drying rate during drying process of agricultural products reduces the energy requirements and the time required for accomplishing drying processes.

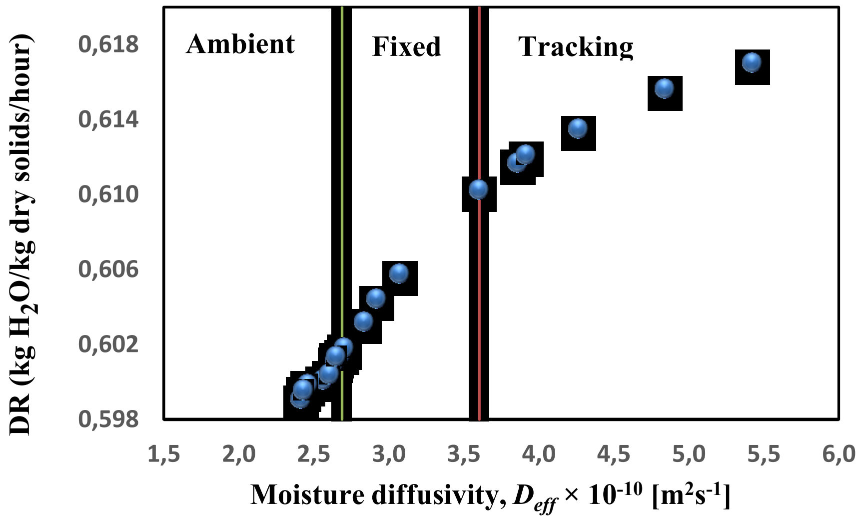

Figure 5. Moisture diffusivity vs. drying rate of apple slices in different drying systems.

3.4. Drying models

Drying data of apple slices expressed as the moisture ratio (*MR*) versus drying time were fitted to **Page** and **Henderson & Pabis** models. As there was no significant difference found between the drying rate of peeled and unpeeled apples slices as explained earlier, drying data were only modeled for unpeeled slices. The drying model constants and the statistical parameters namely the coefficient of determination (R^2), the root mean square error (*RMSE*) and the reduced chi-square (χ^2) used to evaluate the goodness of fit for solar drying of apple slices are listed in Table 5. It is clear from the calculated statistical parameters that both selected models provide a good description of the experimental data under different systems and air flow rates particularly for tracking-based system. It can be also indicated that the Page model gave the higher value of R^2 (0.994) and the lower values of *RMSE* (0.027) and χ^2 (0.0009) for the drying data of the tracking system at the high air flow rate of 44 m^3h^{-1}. Meanwhile, the Henderson & Pabis model gave the highest value of R^2 (0.985) and the lower values of *RMSE* (0.032) and χ^2 (0.0013) for the drying data of the tracking system at the low air flow rate of 22 m^3h^{-1} as shown in Table 5. Based on these results, Both selected models

(**Page model; Henderson & Pabis model**) can be satisfactory describe the drying behavior of apple slice under different drying conditions. These results are in agreement with findings reported by **Velić et al.** (**2004)** and **Kaleta et al. (2013**) who used Page model successfully to describe the drying kinetics of apple. Also, **Zlatanović et al. (2013)** who selected the Henderson & Pabis model as the suitable model to represent the drying characteristics of apple.

Table 5. Statistical results obtained from selected thin-layer drying models of apple slices

Model	$\dot{m}$ (m^3h^{-1})	System	Model constants	R^2	RMSE	χ^2
Page mode $MR = \exp(-kt^n)$	**22**	Tracking	k=0.171; n=1.277	0.983	0.035	0.0015
		Fixed	k=0.1689; n=1.1163	0.973	0.039	0.0019
		Ambient	k=0.1477; n=1.1616	0.972	0.041	0.0021
	33	Tracking	k=0.1525; n=1.3932	0.982	0.038	0.0018
		Fixed	k=0.1603; n=1.1873	0.961	0.051	0.0032
		Ambient	k=0.1476; n=1.1533	0.973	0.040	0.0020
	44	Tracking	k=0.1089; n=1.8159	**0.994**	**0.027**	**0.0009**
		Fixed	k=0.1587; n=1.2414	0.964	0.050	0.0032
		Ambient	k=0.1474; n=1.1631	0.973	0.040	0.0020
			Minimum	**0.961**	**0.027**	**0.0009**
			Maximum	**0.994**	**0.051**	**0.0032**
Henderson & Pabis model $MR = a\exp(-kt)$	**22**	Tracking	a=1.1971; k=0.3054	**0.985**	**0.032**	**0.0013**
		Fixed	a=1.0994; k=0.226	0.978	0.036	0.0016
		Ambient	a=1.1118; k=0.2165	0.976	0.038	0.0018
	33	Tracking	a=1.2512; k=0.3294	0.979	0.039	0.0019
		Fixed	a=1.1565; k=0.2508	0.969	0.045	0.0025
		Ambient	a=1.1043; k=0.2124	0.976	0.038	0.0018
	44	Tracking	a=1.4059; k=0.4175	0.971	0.051	0.0032
		Fixed	a=1.1882; k=0.2734	0.971	0.045	0.0025
		Ambient	a=1.1123; k=0.2167	0.976	0.038	0.0018
			Minimum	**0.969**	**0.032**	**0.0013**
			Maximum	**0.985**	**0.051**	**0.0032**

4. CONCLUSIONS

A solar tracking system was fabricated to be incorporated with a solar air heater manufactured from recyclable aluminum cans (RAC) to enhance its thermal efficiency and to examine its performance in drying apple slices. The tracked solar system enhanced the efficiency of the solar air heater to achieve a maximum efficiency of 87.1% instead of 64.2% for the fixed solar air heater at the same air flow rate. The tracking system increased the moisture diffusivity of apple slices to reach a highest value of 5.43×10^{-10} m^2 s^{-1}. Also, drying rate of apple slices in the tracking system was significantly higher compared with both the fixed system and ambient drying at all tested air flow rates. The drying rate (*DR*) increased with the drying air temperature and flow rate and the highest value of *DR* (0.617 H_2O/kg dry solids/hour) was obtained in the dryer equipped with a tracking module at highest air flow rate of 44 m^3h^{-1}. The results revealed that at the lowest air flow rate of 22 m^3h^{-1}, the drying rate of apple slices was equal for fixed system and ambient air drying. Thus, it can be conclude that the solar air heater is not preferred to be used in drying applications at low air flow rates without enhancing its thermal efficiency using different methods such as tracking system or air circulation. Tracking systems are very effective in providing high values of both moisture diffusivity and drying rate. The high drying rate during drying process of agricultural products reduces the energy requirements and the time required for accomplishing drying processes.

Acknowledgements

Authors significantly acknowledge the financial support from the Marie Sklodowska-Curie COFUND P-SPHERE project under the European Union's Horizon 2020 research and innovation programme with grant agreement No665919 and the Distinguished Scientist Fellowship Program (DSFP), King Saud University.

5. REFERENCES

Akpinar, E. K., Bicer, Y., & Yildiz, C. (2003). Thin layer drying of red pepper. Journal of Food Engineering, 59(1), 99–104.

Alta D., Bilgili E., Ertekin C. and Yaldiz O. (2010). Experimental investigation of three different solar air heaters: Energy and exergy analyses. Applied Energy, 87:2953-2973.

Alvarez G., Arce J., Lira L. and Heras M. (2004). Thermal performance of an air solar collector with an absorber plate made of recyclable aluminum cans. Solar Energy, 77:107-113.

Amer B., Hossain M. and Gottschalk K. (2010). Design and performance evaluation of a new hybrid solar dryer for banana. Energy conversion and management ,51:813-820.

Anusha, K.; Chandra, S. and Mohan, R. (2013). Design and development of real time clock based efficient solar tracker system. International journal of Engineering Research and Applications (IJERA), 3, 1219-1223.

Anyaka, B. O.; Ahiabuike, D. C. and Mbunwe, M. J. (2013). Improvement of PV Systems Power Output Using Sun-Tracking Techniques. International Journal of Computational Engineering Research, 3, 80-98.

Banerjee, R. (2015). Solar Tracking System. International Journal of Scientific and Research Publications, 5 (3) 2250-3153.

Baroni, A. F. and Hubinger, M. D. (1998). Drying of onion: effects of pretretmant on moisture transport. Drying Technology, 16(9&10), 2083–2094.

Bione, J.; Vilela, O. C. and Fraidenraich, N. (2004). Comparison of the performance of PV water pumping systems driven by fixed, tracking and V-trough generators. Solar energy, 76, 703-11.

Brooks M., El-Hana N.A. and Ghaly A. (2008). Effects of tomato geometries and air temperature on the drying behavior of plum tomato. American Journal of Applied Sciences, 5:1369-1375.

Clifford, M. J. and Eastwood, D. (2004). Design of a novel passive solar tracker. Solar Energy, 77, 269-280.

Defraeye, T. and Radu, A. (2018). Insights in convective drying of fruit by coupled modeling of fruit drying, deformation, quality evolution and convective exchange with the airflow. Applied Thermal Engineering, 129, 1026-1038.

Devan, P. K., Bibin, C., Gowtham, S., Hariharan, G., & Hariharan, R. (2020). A comprehensive review on solar cooker with sun tracking system. Materials Today Proceedings. (In Press). https://doi.org/10.1016/j.matpr.2020.06.124

Dhanabal, R.; Bharathi, V.; Ranjitha, R.; Ponni, A.; Deepthi, S. and Mageshkannan, P. (2013). Comparison of efficiencies of solar tracker systems with static panel single axis tracking system and dual axis tracking system with fixed mount. International Journal of Engineering and Technology (IJET), 5, 1925-1933.

Diamante, L. M. (1994). Drying characteristics of sweet potato slices. In Proceedings of the international conference of preservation and security (pp. 187-199).

Doymaz I. (2007). Air-drying characteristics of tomatoes. Journal of Food Engineering, 78:1291-1297.

Doymaz, I. and Pala, M. (2003). The thin-layer drying characteristics of corn. Journal of Food Engineering, 60, 125-130

ElGamal R., Ronsse F., ElMasry G. and Pieters J.G. (2015). Development of a Multi-Scale Model for Deep-Bed Drying of Rice. Transactions of the ASABE, 58: 849-859.

ElGamal R., Ronsse F., Radwan S.M. and Pieters J.G. (2014). Coupling CFD and Diffusion Models for Analyzing the Convective Drying Behavior of a Single Rice Kernel. Drying Technology, 32:311-320.

Guihua, Li.; Runsheng, T. and Hao, Z. (2012). Optical Performance of Horizontal Single Axis tracked Solar Panels. International Conference on Future Energy, Environment and materials, 16, 1744-1752.

Kaleta, A., Górnicki, K., Winiczenko, R. and Chojnacka, A. (2013). Evaluation of drying models of apple (var. Ligol) dried in a fluidized bed dryer. Energy Conversion and Management, 67, 179-185.

Kaya, A., Aydin, O. and Demirtas, C. (2007). Drying kinetics of red delicious apple. Biosystems Engineering, 96, 517-524.

Khan, M. T. A.; Tanzil, S. M. S.; Rahman, R. and Alam, S. M. S. (2010). Design and Construction of an Automatic Solar Tracking System. 6th International Conference on Electrical and Computer Engineering, 18 – 20 December, Dhaka, Bangladesh.

Kishk, S. S., ElGamal, R. A. and ElMasry, G. M. (2019). Effectiveness of recyclable aluminum cans in fabricating an efficient solar collector for drying agricultural products. Renewable energy, 133, 307-316.

Marcel, S.; Tomas, C.; Artur, S. and Juraj, B. (2012). Solar electricity production from fixed-inclined and sun-tracking photovoltaic modules in South Africa." 1st Southern African Solar Energy Conference (SASEC), 1-8.

Miloudi, L.; Acheli, D. and Ahmed, C. (2013). Solar tracking with photovoltaic system. Energy Procedia, 42, 103-112.

Mork, B. A. and Weaver, W. W. (2009). Smart Grids and Micro Grids, where are they really. Minnesota Power Systems Conference, 3 -5 November, Brooklyn Center, MN, USA.

Ozgen F., Esen M., Esen H. (2009). Experimental investigation of thermal performance of a double-flow solar air heater having aluminium cans. Renewable Energy, 34:2391-2398.

Pizzocaro, F., Torreggiani, D. and Gilardi, G. (1993). Inhibition of apple polyphenoloxidase (PPO) by ascorbic acid, citric acid and sodium chloride. Journal of Food Processing and Preservation, 17(1), 21-30.

Quesada, G.; Guillon, L.; Rousse, D.; Mehrtash, M.; Dutil, Y. and Paradis, P. L. (2015). Tracking strategy for photovoltaic solar systems in high latitudes. Energy Conversion and Management, 103, 147-156.

Rao, V. B.; Kumar, K. D. H.; Kumar, N. V. U. and Deepak, K. (2017). Arduino based two axis solar tracking by using servo mechanism. International Journal for Modern Trends in Science and Technology, 3(2), 41-44.

Rizk, J. and Chaiko,Y. (2008). Solar Tracking System- More Efficient Use of Solar Panels." World Academy of Science, Engineering and Technology, 17,313-315.

Sacilik K., Keskin R. and Elicin A.K. (2006). Mathematical modelling of solar tunnel drying of thin layer organic tomato. Journal of food Engineering, 73:231-238.

Samimi-Akhijahani, H., & Arabhosseini, A. (2018). Accelerating drying process of tomato slices in a PV-assisted solar dryer using a sun tracking system. Renewable Energy, 123, 428-438.

Santos B., Queiroz M. and Borges T. (2005). A solar collector design procedure for crop drying. Brazilian Journal of Chemical Engineering, 22:277-284.

Sekyere C.K.K., Forson F.K. and Adam F.W. (2016). Experimental investigation of the drying characteristics of a mixed mode natural convection solar crop dryer with back up heater. Renewable Energy, 92, 532-542.

Snehal, H. P. and Kolte, M. T. (2013). FPGA Based Standalone Solar Tracking System. International Journal of Scientific and Research Publications, l3, 1-5.

Sreekumar A. (2010). Techno-economic analysis of a roof-integrated solar air heating system for drying fruit and vegetables. Energy Conversion and Management ,51:2230-2238.

Sreekumar A., Manikantan P. and Vijayakumar K. (2008). Performance of indirect solar cabinet dryer. Energy Conversion and Management, 49:1388-1395.

Tiberiu, T.; Constantin, D. O. and Lliviu, K. (2012). Performance evaluation of a solar tracking PV panel." U.P.B. Sci. Bull series C 74:3-10.

Tutuncu, M. A. and Labuza, T. P. (1996). Effect of geometry on the effective moisture transfer diffusion coefficient. Journal of Food Engineering, 30, 433-447.

Vega-Gálvez, A., Ah-Hen, K., Chacana, M., Vergara, J., Martínez-Monzó, J., García-Segovia, P., ... and Di Scala, K. (2012). Effect of temperature and air velocity on drying kinetics, antioxidant capacity, total phenolic content, colour, texture and microstructure of apple (var. Granny Smith) slices. Food Chemistry, 132(1), 51-59.

Velić, D., Planinic, M., Tomas, S., and Bilic, M. (2004). Influence of airflow velocity on kinetics of convection apple drying. Journal of Food Engineering, 64, 97-102.

Watane, N. D. and Dafde, R. A. (2013). Automatic solar tracker system. International Journal of Scientific & Engineering Research, 4 (6), 93-100.

Yousef, H. A. (1999). Design and implementation of a fuzzy logic computer-controlled sun tracking system. In Proceedings of IEEE International Symposium on Industrial Electronics, Bled, Slovenia, Jul. 12-16.

Zlatanović, I., Komatina, M. and Antonijević, D. (2013). Low-temperature convective drying of apple cubes. Applied Thermal Engineering, 53(1), 114-123.